Adaptive Backstepping Control Design for ATMD systems in Nonlinear Structures with Nonlinear Disturbance and Parametric Uncertainties

Rafet Can Ümütlü [1*], Baris Bidikli [2], Hasan Ozturk [3], Aleksandar Pavic[4]

[1] TOFAŞ Turkish Automobile Factory Joint-Stock Company, R&D, Propulsion Systems, Bursa, Türkiye

[2] Department of Mechatronics Engineering, Faculty of Engineering and Architecture, Izmir Katip Celebi University, Izmir, Türkiye

[3] Department of Mechanical Engineering, Faculty of Engineering, Dokuz Eylul University, Tinaztepe, Buca, Izmir, Türkiye

[4] College of Engineering, Mathematics and Physical Sciences, Vibration Engineering Section, University of Exeter, North Park Road, Exeter EX4 4QF, UK

E-mail: [1]*rafet.canumutlu@tofas.com.tr*, [2]*baris.bidikli@ikcu.edu.tr*, [3]*hasan.ozturk@deu.edu.tr*, [4]*A.Pavic@exeter.ac.uk*

Abstract

Active tuned mass damper (ATMD) devices are recommended in various structures to reduce vibrations. The performance of the ATMD system is closely tied to the control design utilized, according to research in the literature. The designed control input will take into account as much system dynamics as possible, making it possible to use it as a generalized controller in all similar systems. Nonlinear behavior is the natural behavior of engineering structures and in order to obtain a more realistic and high-performance ATMD system, it can be considered as an appropriate approach to design the controller by considering the structural nonlinearities. In addition, unexpected external influences and parameter uncertainties must be taken into account during control design to ensure that control systems perform successfully in similar systems in all conditions. Therefore, in this study, the nonlinear model of the multi-story building was reconstructed by adding nonlinear disturbance to represent unknown external effects. Band limited white noise is used as a disturbance function and gaussian white noise is added to measured states in this study. To obtain a robust controller, unknown structural parameters are compensated for by using adaptive compensation terms. With the controller design supported by Lyapunov-based stability analysis, the stability of the vibrating structure featuring ATMD is theoretically guaranteed while achieving the main control goal. Performance analyses of the designed controllers are carried out with simulation studies. The efficiency of the developed

*Corresponding author: Rafet Can Ümütlü
E-mail address: rafet.canumutlu@tofas.com.tr

Lyapunov-based controller in dampening the unwanted vibrations that occurred on the building is seen in simulation results.

Keywords: *ATMD, Robust Adaptive Backstepping Control, Lyapunov-Based Control, Nonlinear Control, Vibration Control*

Funding Acknowledgement: The authors would like to acknowledge the support of the Scientific and Technological Research Council of Turkey (TUBITAK) 2214-A International Doctoral Research Fellowship Programme.

Conflict of interest statement: The authors declare no conflict of interest in preparing this article

1. Introduction

The structural vibrations created by earthquakes pose a serious hazard to both structures and people. Many control studies have been carried out under the topic of vibration control in order to counteract this threat. This subject has maintained its place and relevance on the agenda in recent years. Studies to reduce earthquake-induced vibrations may be divided into two categories: passive and active vibration control approaches.

Tuned mass damper (TMD) systems are one of the most widely used passive vibration damping methods. The main purpose of such vibration control studies is to dampen the unwanted vibrations of the building during an earthquake by producing a reverse vibration response. The working principle of TMD systems is based on core knowledge. This principle consists of a mostly single degree of freedom mass spring damper system that transfers and absorbs the kinetic energy of the structure onto itself (Preumont et al., 2014). By incorporating the actuator in the traditional TMD system, an active tuned mass damper (ATMD) is created. The fact that ATMD provides better outcomes than TMD and requires a lower control mass is seen as the active form of traditional TMD systems, which makes it beneficial when it comes to utilize ATMD over the passive approach. Usually located on the top floor, the ATMD acts via the specified control signal, creating a vibration response and reducing the overall response of the building's vibration (Yu & Thenozhi, 2016). Because multi-degree-of-freedom systems vibrate in many vibrational modes, ATMD systems work extremely well to dampen the vibrations of such structures (Collette & Chesné, 2016). Controller design is a very important process in systems where active controllers are used for vibration control. Reducing the control effort required, especially during vibration reduction, is the main point of most studies. ATMD systems and different control approaches are used together to mitigate the earthquake-related vibrations in the structures. Adhikari *et al.* studied on sliding mode controller (SMC) design for ATMD systems that dampen the vibration of a high buildings (Adhikari et al., 1998). The most extensively utilized controller for ATMD systems is the proportional integral derivative (PID) controller. (Etedali et al., 2018; Etedali & Tavakoli, 2017; Kayabekir et al., 2020). The PID controller was widely preferred when there was a need for performance comparison with other controllers in the developed control studies (Guclu, 2006; Kayabekir et al., 2020; Ümütlü et al., 2021). Guclu & Yazici, (2008) used both active base isolator and ATMD in the study. They used a fuzzy logic controller to dampen the vibrations of a 15-story structure and compared the performance of the controller with that of the PID controller. Li & Cao, (2019) for the design of an ATMD system, combined dynamic magnification factors of the structure with particle swarm optimization.

In the structural control studies carried out in the literature, building structures have been modeled linearly, which is a very common approach. But physical system models typically incorporate various kinds of uncertainty. These uncertainties generally arise from material and geometric nonlinearities, but also from possible uncertain external effects like measurement noise, unmodeled dynamics and etc. Nonlinear behavior is the natural behavior of multi-story buildings with ATMD systems. Therefore, studying nonlinearity in structural systems has been a necessary area of research in recent years. Along with these studies, vibration reduction and performance improvement of nonlinear systems under major earthquakes has recently attracted the attention of researchers (Aghabalaei Baghaei et al., 2019). For this reason, a large number of controllers have been designed to be used with various vibration dampening systems in models containing various nonlinearities. However, in buildings where nonlinear models are used, which have increased in recent years, linear building models placed on a nonlinear base isolator are often preferred instead of using a completely nonlinear structure.

Nonlinear systems have complex behavior when compared to linear systems. Numerous nonlinear models have been developed by researchers to model these complex behaviors. The Duffing oscillator, which is a second-order differential equation with nonlinear cubic stiffness, is often preferred in nonlinear problems (Alexander & Schilder, 2009; Chang & Poon, 2010; Eason et al., 2013; Ghandchi Tehrani & Elliott, 2014; Mañosa et al., 2005). One of the characteristic features of a Duffing oscillator is its chaotic behavior tendency when forced by a periodic force (Fang et al., 2001; Ghandchi-Tehrani et al., 2015; Novak & Frehlich, 1982). In addition to the difficulty of dealing mathematically with typical nonlinear systems, these types of systems are equally challenging to control. To overcome this difficulty, various linearization approaches such as feedback linearization, linearization around equilibrium points and etc. have been used in vibration control studies for nonlinear modeled structures(Anh & Nguyen, 2012; Ghaffarzadeh et al., 2020; Socha & Blachuta, 2000). To improve the performance of nonlinear duffing systems exposed to nonstationary random excitations, Aghabalaei Baghaei et al., (2019) applied equivalent linearization (EL) and SMC techniques. As a result of this linearization, linear control strategies are used for ATMD systems. However, while designing controllers for a structure with nonlinear dynamics, it is seen as a more realistic approach to design a nonlinear controller.

In controller design for ATMD systems, it is a critical strategy to create a controller that just requires system states. Because a controller design based on the assumption that the system parameters are completely or partially known is not a practical approach when it comes to a construction system. ATMD systems, which are used for damping structural vibrations, are very useful systems not only for new structures but also for existing structures. In particular, it is not possible to estimate the system parameters of existing structures with absolute accuracy. A controller design that includes system parameters is very inefficient when these values cannot be used correctly. It even has the potential to be dangerous by increasing vibration and producing control responses that can cause resonance. In addition, a control design free from system parameters will be in a generalized form that can be used not only for a single structure, but also for all structures with the same mathematical model. Considering the aforementioned cases, it seems that system parameters free control design is appropriate for this type of system.

A vital point that should not be neglected in the design of the controller for ATMD systems is to support the controller with a stability analysis that guarantees the stability of the system. When controller designs whose stability is not mathematically guaranteed are used in such ATMD systems, the system may be unstable due to the control input effect. This situation can be more harmful for the structure than an earthquake. In this case, it should theoretically be assured that the proposed controller can achieve zero convergence of all structural states and ensure the overall system's stability during the control process.

The major aim of this research is to develop a controller that can dampen earthquake-induced vibrations in a nonlinear structure using ATMD systems without relying on system characteristics. It is aimed to eliminate parametric uncertainties by employing compensation terms that are recommended based on the existing system circumstances. Another motivation for this approach is that controllers equipped with such compensation rules require much less control effort than traditional robust controller designs for nonlinear structures, as evidenced many times in the control literature to control various linear systems. Considering its appropriateness for these types of vibration control work, a backstepping control method was used in the controller design. It is theoretically supported by Lyapunov-based arguments to show that the developed controller can achieve zero convergence of all fundamental displacements and maintain system stability throughout the control process. A nonlinear nine-story building model that was subjected to a severe earthquake was utilized for the simulation studies of the proposed controller. Some full-scale implementations of ATMD systems used in buildings can be given an example Kyobashi Center (11-story), Shimizu Tech Lab (7-story), and Ando Nishikicho Building (14-story) (Gutierrez Soto & Adeli, 2013). Band-limited white noise has been added to the system equation of the structure as a disturbance function. Matlab/Simulink was used to conduct the simulation studies required for this research.

2. MDOF Duffing Structure System

The mathematical model of N story shear type duffing structure is given below,

$$\mathbf{M}\ddot{\mathbf{y}}(t) + \mathbf{C}\dot{\mathbf{y}}(t) + \mathbf{K}\mathbf{y}(t) + \mathbf{G}(t) + \boldsymbol{\psi} f_d = 0 \tag{1}$$

where $\mathbf{M} \in \mathbb{R}^{n\times n}$, $\mathbf{C} \in \mathbb{R}^{n\times n}$ and $\mathbf{K} \in \mathbb{R}^{n\times n}$ represent mass, damping and stiffness coefficient matrixes, respectively. f_d is the nonlinear disturbance term and $\boldsymbol{\psi} = [\mathbf{0}\ \mathbf{0} \ldots \mathbf{0}\ \mathbf{1}]^{\boldsymbol{T}}$ is the (nxn) orientation vector for the nonlinear disturbance. $\mathbf{G}(t) \in \mathbb{R}^{n\times n}$ is the nonlinear term vector. $\mathbf{y}(t) = [\boldsymbol{y_0}\ \boldsymbol{y_1} \ldots \boldsymbol{y_{n-1}}\ \boldsymbol{y_n}]^{\boldsymbol{T}}$ is the displacement vector and each element of this vector represent the related floor displacement. $\dot{\mathbf{y}}(t)$ and $\ddot{\mathbf{y}}(t)$ are first and second-time derivatives of the displacement vector. They represent the velocity vector and acceleration vector, respectively. The earthquake-induced ground motion is indicated by $y_0 \in \mathbb{R}$, and its first time derivative is the velocity of the ground motion is represented by $\dot{y}_0 \in \mathbb{R}$.

$$\mathbf{G}(t) = \begin{bmatrix} \alpha_1 k_1 x_1^3 - \alpha_2 k_2 x_2^3 \\ \alpha_2 k_2 x_2^3 - \alpha_3 k_3 x_3^3 \\ \alpha_3 k_3 x_3^3 - \alpha_4 k_4 x_4^3 \\ \vdots \\ \alpha_{n-1} k_{n-1} x_{n-1}^3 - \alpha_n k_n x_n^3 \\ \alpha_n k_n x_n^3 \end{bmatrix}; \quad \begin{bmatrix} x_1 \\ x_2 \\ x_3 \\ \vdots \\ x_{n-1} \\ x_n \end{bmatrix} = \begin{bmatrix} y_1 - y_0 \\ y_2 - y_1 \\ y_3 - y_2 \\ \vdots \\ y_{n-1} - y_{n-2} \\ y_n - y_{n-1} \end{bmatrix} \tag{2}$$

The extended mathematical model of the top floor and control mass when a nonlinear optimum ATMD is installed on the top floor of the NDOF shear nonlinear building structure, described in Eq. 1 and Eq. 2, for vibration control purposes is as follows.

$$m_n\ddot{y}_n + b_n(\dot{y}_n - \dot{y}_{n-1}) - b_d(\dot{y}_d - \dot{y}_n) + k_n\alpha_n(y_n - y_{n-1}) + k_n(1-\alpha_n)(y_n - y_{n-1})^3 - k_d\alpha_d(y_d - y_n) - k_d(1-\alpha_d)(y_d - y_n)^3 + f_d = u_f \quad (3)$$

$$m_d\ddot{y}_d + b_d(\dot{y}_d - \dot{y}_n) + k_d\alpha_d(y_d - y_n) + k_d(1-\alpha_d)(y_d - y_n)^3 = -u_f \quad (4)$$

where $m_d \in \mathbb{R}$ represents mass coefficient, $k_d \in \mathbb{R}$ represents stiffness coefficient and $b_d \in \mathbb{R}$ represents the damping coefficient for the ATMD system.

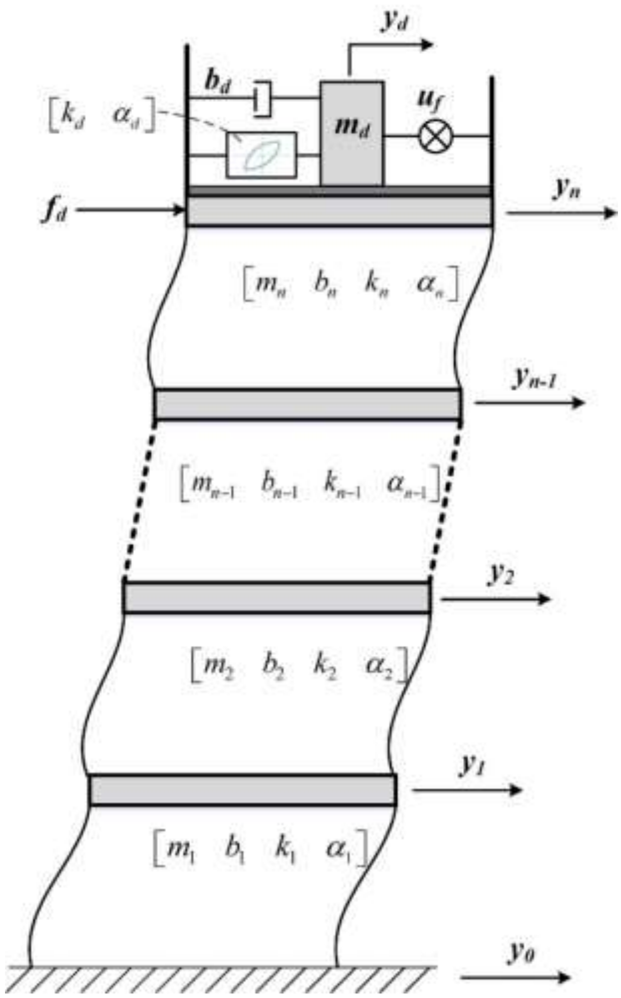

Figure 1. Model of nonlinear structure with nonlinear ATMD

In Eq. (3) and Eq. (4) $m_n \in \mathbb{R}$ represents mass coefficient, $k_n \in \mathbb{R}$ represents stiffness coefficient, $b_n \in \mathbb{R}$ represents damping coefficient, and $\alpha_n \in \mathbb{R}$ represents nonlinearity coefficient for the last floor. $y_j \in \mathbb{R}$ and first and second-time derivatives of the displacement represent the related floor's velocity and acceleration. As shown in the Figure 1, the ATMD system features a tuned moveable mass whose movement is controlled by force input denoted by $u_f \in \mathbb{R}$. The specified controller mass moves in the horizontal axis as a consequence of the common action of spring and damping components and the applied force, and this movement is represented by displacement denoted by $y_d \in \mathbb{R}$.

In the aforementioned model, the mass coefficient $m_d \in \mathbb{R}$, stiffness coefficient $k_d \in \mathbb{R}$, damping coefficient $b_d \in \mathbb{R}$, and nonlinearity coefficient $\alpha_d \in \mathbb{R}$ are used to represent this movement mathematically. The ground motion caused by an earthquake is indicated by $y_0 \in \mathbb{R}$, and the velocity is represented by its first time derivative.

3. Controller Design for ATMD systems Using in Nonlinear Structures

The control design and Lyapunov based stability analysis of closed loop system proposed in this section are based on the representation of multi-story nonlinear buildings controlled by the ATMD system against seismic vibrations with a generalized model similar to the system model.

$$\dot{x} = \dot{\xi}_n \tag{5}$$

$$p_1\ddot{\xi}_n = f\left(\xi_{n-1}, \xi_n, \xi_{n+1}, \xi_{n-1}^3, \xi_n^3, \xi_{n+1}^3, \dot{\xi}_{n-1}, \dot{\xi}_n, \dot{\xi}_{n+1}\right) + f_d - u_f \tag{6}$$

where $x, \xi_{n+1}, \xi_n, \xi_{n-1} \in \mathbb{R}$ and their first and second time derivatives denote the system states, n denotes degree-of-freedom of the system, f is a function that contains nonlinear arguments of system states effective on system dynamics, f_d is the nonlinear disturbance term, u_f represents the control force, and $p_1 \in \mathbb{R}$ denotes the constant system parameters.

Property 1. The term f can be linearly parametrized as

$$f = Y_d\phi \tag{7}$$

where, $Y_d\left(\xi_{n-1}, \xi_n, \xi_{n+1}, \dot{\xi}_{n-1}, \dot{\xi}_n, \dot{\xi}_{n+1}\right) \in \mathbb{R}^{1xl}$ is the system state vector and $\phi \in \mathbb{R}^{lx1}$ is the represents uncertain constant parameter vector of system. All elements of vector Y_d are available.

The adaptive compensation term represented by $\hat{\phi} \in \mathbb{R}$ ensure the robustness of the designed controller. A Compensation error term is needed to show the difference between the system parameters and the adaptive compensation term. The compensation error is defined as follows

$$\tilde{\phi} \triangleq \hat{\phi} - \phi \tag{8}$$

The auxiliary error defined as

$$e \triangleq u_v - \dot{\xi}_n \tag{9}$$

Virtual controller designed as

$$u_v \triangleq -G_1 x \tag{10}$$

where $G_1 \in \mathbb{R}^+$ represents constant positive definite gain of virtual controller. The first close loop system is completed by the virtual controller substituting for the system state to be controlled in Eq. (5).

$$\dot{x} = -G_1 x \tag{11}$$

The time derivative of Eq. 9 is multiplied by p_1. Substituting Eq. 6 and Eq. 10 in the obtained equation, the following equation is obtained.

$$p_1 \dot{e} = -p_1 G_1 \dot{\xi}_n + Y_d \phi + f_d - u_f \tag{12}$$

Adaptive compensations of uncertain system parameters are used to deal with parametric uncertainty. The adaptive compensation errors $\tilde{p}_1$ and $\tilde{\phi}$ show the errors between adaptive compensation terms $\hat{p}_1$and $\hat{\phi}$ uncertain system parameters $p_1$and ϕ.

$$\tilde{p}_1 = \hat{p}_1 - p_1 \tag{13}$$

$$\tilde{\phi} = \hat{\phi} - \phi \tag{14}$$

Eq. 13 and Eq. 14 are substituted in Eq. 12.

$$p_1 \dot{e} = (\tilde{p}_1 - \hat{p}_1) G_1 \dot{\xi}_n + Y_d \left(\hat{\phi} - \tilde{\phi} \right) + f_d - u_f \tag{15}$$

The control function is designed according to Eq. 15.

$$u_f = -\hat{p}_1 G_1 \dot{\xi}_n + Y_d \hat{\phi} + \rho_e tan\, h(e) + G_2 e \tag{16}$$

where $G_2 \in \mathbb{R}^+$ is constant positive definite control gain. Eq. 16 are substituted in Eq. 15.

$$p_1 \dot{e} = \tilde{p}_1 G_1 \dot{\xi}_n - Y_d \tilde{\phi} + f_d - \rho_e tanh\, (e) - G_2 e \tag{17}$$

Lyapunov-based stability analysis is performed to obtain semi-global asymptotic convergence of the error terms defined in the closed-loop system. The nonnegative Lyapunov function $V(x, e, \tilde{p}_1, \tilde{\phi})$ is defined as

$$V \triangleq \frac{1}{2} x^2 + \frac{1}{2} p_1 e^2 + \frac{1}{2} \tilde{\phi}^T \tilde{\phi} + \frac{1}{2} \tilde{p}_1{}^2 \tag{18}$$

Time derivative of Eq. (15) is obtained in the following form when Eq. (4), Eq. (9), and Eq. (14) are utilized

$$\dot{V} = -G_1x^2 - G_2e^2 + \tilde{\phi}^T\left(\dot{\hat{\phi}} - Y_d^T e\right) + \tilde{p}_1(\dot{\hat{p}}_1 + eG_1\dot{\xi}_n)$$
$$+ e(f_d - \rho_e tanh\,(e)) \tag{19}$$

If adaptive compensations of uncertain parameters are made according to the following rules, the Lyapunov stability criterion in Eq. (19) is guaranteed.

$$\dot{\hat{\phi}} = Y_d^T e \tag{20}$$

$$\dot{\hat{p}}_1 = -eG_1\dot{\xi}_n \tag{21}$$

$$\rho_e \geq max(f_d) \tag{22}$$

Using Eq. (20), Eq. (21) and Eq. (22), the time derivative of Lyapunov function in Eq. (19) can be rearranged

$$\dot{V} = -G_1x^2 - G_2e^2 \tag{23}$$

From the Eq. (23), it can be demonstrated that time derivative of the Lyapunov function can be upper bounded as

$$\dot{V} \leq -\beta\|\mathbf{z}\|^2 \tag{24}$$

where $\mathbf{z} \in \mathbb{R}^2$ is a vector defined as

$$\mathbf{z} \triangleq [x \quad e]^T \tag{25}$$

and $\beta \in \mathbb{R}^+$ denotes a positive constant selected as

$$\beta = \min\{g_1, g_2\} \tag{26}$$

Lyapunov function Eq. (18) and the bound of time derivative of Lyapunov function Eq. (24) it is seen that $\mathbf{z}(t) \in \mathcal{L}_\infty$. Boundedness of this term guarantees the boundedness of x and e. From virtual controller design in Eq. (10), it is seen that boundedness of x guarantees the boundedness of u_v. The virtual control input's boundedness, as well as the boundedness of e and its definition in Eq. (9), can be used together to show that $\dot{\xi}_n \in \mathcal{L}_\infty$. When boundedness of $\dot{\xi}_n$ is utilized along with Eq (5) and the time derivative of Eq (11) to show that $\ddot{\xi}_n \in \mathcal{L}_\infty$ and can be utilized with the time derivative of Eq (10) to show that $\dot{u}_v \in \mathcal{L}_\infty$. Boundedness of time derivative of virtual controller and boundedness of $\ddot{\xi}_n$ can be used along with the time derivative of error function to show that $\dot{e} \in \mathcal{L}_\infty$. Boundedness of $\dot{\xi}_n$ and $\dot{e}$ ensures that $\dot{z}(t)$ is also bounded.

$$\int_0^\infty \|\mathbf{z}(\sigma)\|^2 d\sigma \leq \frac{V(0)}{\beta}. \tag{27}$$

The boundedness of the $\dot{\mathbf{z}}(t) \in \mathcal{L}_\infty$, together with $\mathbf{z}(t) \in \mathcal{L}_2 \cap \mathcal{L}_\infty$ and Barbalat's Lemma (Krstic et al., 1995), can be used to show semi-global asymptotic stability of z(t), which assures the main aim of the control design defined as

$$x, e \to 0 \text{ as } t \to \infty \tag{28}$$

4. Numerical Studies

The numerical parameters of the nine-story building model used in the simulation studies were taken from a translational type linear structure used in the literature. This structure is nonlinearized according to the duffing nonlinearity rules, and this nonlinearity is explained in Eq. 1 to Eq. 4. In the non-linear structure, instead of the TMD damper used in the literature, Optimal TMD with the same mass as the original TMD (Hacioglu & Yagiz, 2012; Ümütlü et al., 2022) and much better performance is used. Calculations for optimal TMD are taken from Krenk, (2005). The original TMD and optimal TMD results are compared in Figure 3. Optimal TMD, which has a much better performance than the original TMD, was activated and used as ATMD in the study.

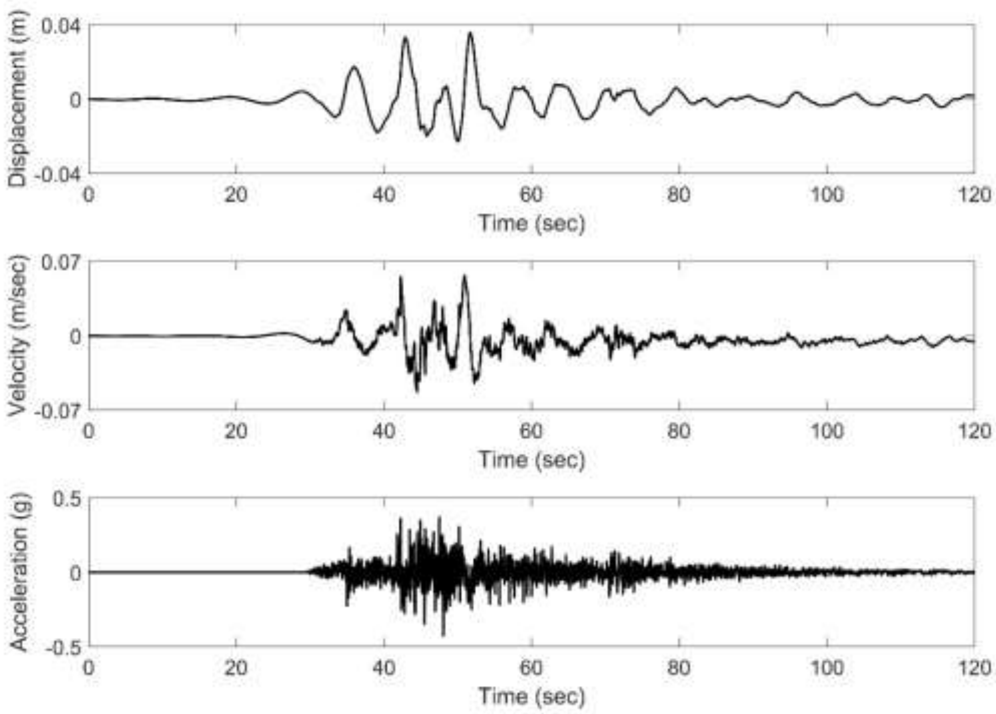

Figure 2. Acceleration, velocity and displacement data of Kocaeli Earthquake

The nonlinear structure and the nonlinear optimal TMD parameters are given in Table 1 . The determined structure was exposed to the 17 August 1999 Kocaeli earthquake in Turkey. The acceleration, velocity, and displacement of the ground motion are shown in Figure 2.

Table 1. Parameters of the nonlinear building model and the nonlinear ATMD (Hacioglu & Yagiz, 2012)

Parameter	Value×10^3 (kg)	Parameter	Value×10^6 (N/m)	Parameter	Value×10^3 (Ns/m)	Parameter	Value
m_1	450	k_1	18.05	b_1	26.17	α_1	0.6
m_2	345	k_2	340	b_2	490	α_2	0.5
m_3	345	k_3	326	b_3	467	α_3	0.5
m_4	345	k_4	285	b_4	410	α_4	0.5
m_5	345	k_5	269	b_5	386	α_5	0.5
m_6	345	k_6	243	b_6	348	α_6	0.5
m_7	345	k_7	207	b_7	298	α_7	0.5
m_8	345	k_8	169	b_8	243	α_8	0.5
m_9	345	k_9	137	b_9	196	α_9	0.5
m_d	69	k_d	0.31954	b_d	33.553	α_d	0.5

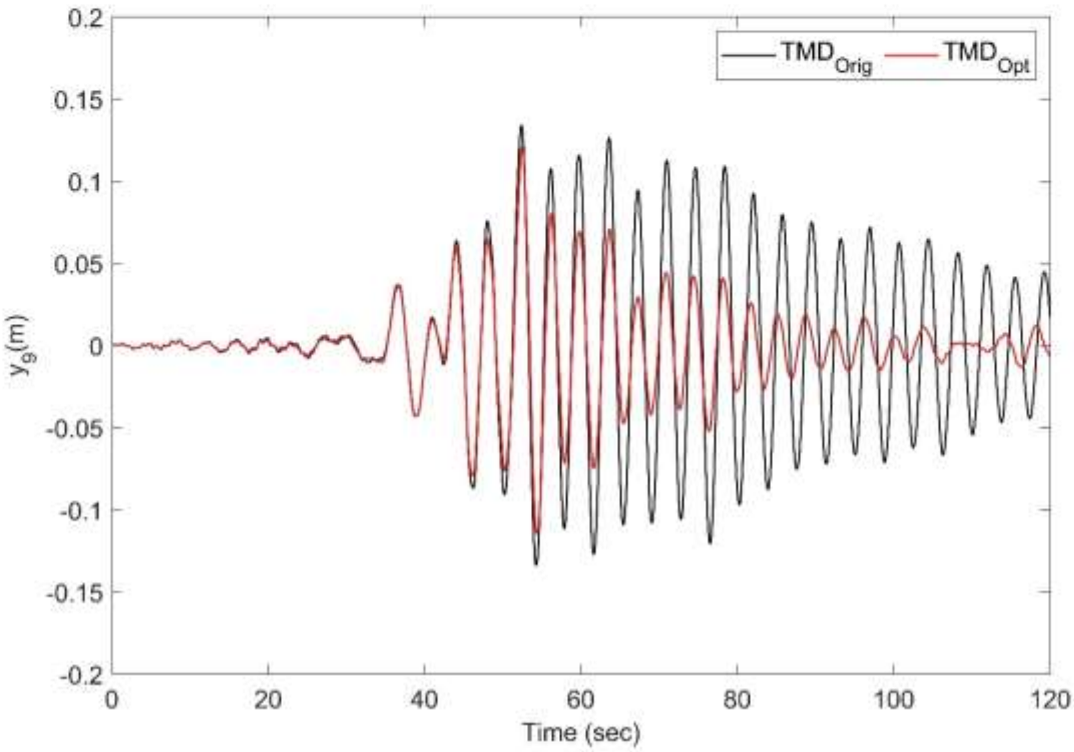

Figure 3. Comparison of original TMD and optimal TMD against the Kocaeli earthquake

The optimal TMD design with the same mass as the original TMD design showed a great performance improvement as shown in Figure 3. The passive controller, to which the robust adaptive controller designed within the scope of this study will be compared, has reached the best point it can be reached with the optimal TMD design. The point that should not be forgotten here is that due to the structure of optimal TMD design, gives these types of successful results only for the proposed structure. When the structural parameters are changed, its performance will be adversely affected. However, it would be more accurate to compare the controller designed to reduce vibration in nonlinear structures with the optimal TMD, in order to ensure adequate comparison.

In this study, a signal-to-noise ratio of 50 dB is chosen for the band-limited white noise used for the white noise added to the sensors. The gains are selected as follows via trial and error method and the designed controller in Eq. (16) is applied from the actuator input of ATMD system

$$G_1 = 100, G_2 = 6000, \rho_e = 5 \tag{24}$$

It should be mentioned at this time that as the control gains values are increased while determining the gains, the ATMD performance improves, but the control effort and stroke of the control mass also increased. In light of this, the control gain adjustment procedure was stopped at the final position when ATMD performance greatly improved, and the control gains were acquired as shown in Eq. (24). Following this point, the control effort and displacement of the control mass increased as the control gains increased, while the ATMD performance remained similar. It has been demonstrated that the suggested controller may be used in such structures if the control gains are chosen to be positive definite in order to meet the main control goal.

Figure 4 shows the displacement of the last floor of a nine-story nonlinear structure for three different control situations during the Kocaeli earthquake. These situations are referred uncontrolled, optimal TMD control and ATMD control situations. Optimal TMD is used in the ATMD system by activating it with an actuator. As can be easily understood from the figure, it has been observed that better results can be obtained in the final floor displacements of the building compared to an uncontrolled situation by using the TMD system. However, the amplitude of the displacement in each period during the earthquake and the time it takes to reduce the residual vibrations are considerably lower when the ATMD system is used with the designed adaptive backstepping controller compared to the case when TMD is used. It is seen that the designed controller, a nonlinear ATMD system, significantly reduces earthquake-induced oscillations occurring on the top floor of a nonlinear structure.

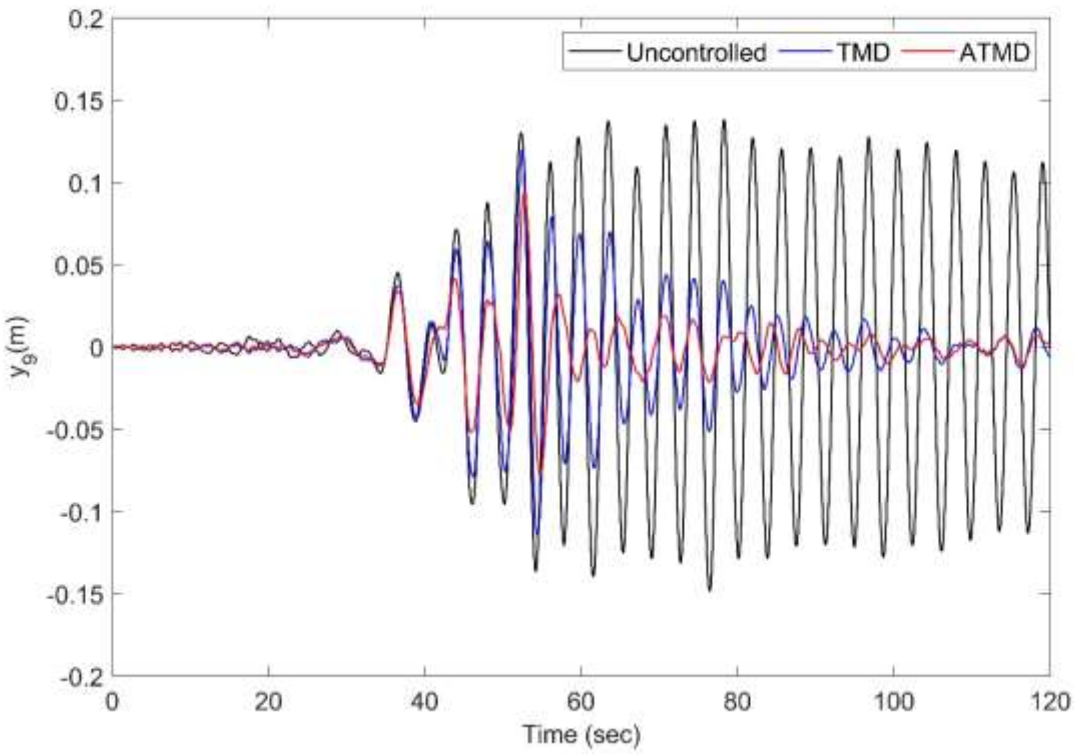

Figure 4. Displacement of the last floor of the structure for three different situations

The designed controller's performance was compared to that of its robust counterpart. For purposes of comparison, PID controllers were selected. The key justification for this choice was that the PID controller is frequently used in systems of this kind. Until the highest vibration damping performance was attained, the proportional (P), integral (I), and derivative (D) control gains of the PID controller were selected as follows via the trial-and-error method until the best vibration damping performance was obtained

$$P = 1000000, I = 1000, D = 950 \tag{33}$$

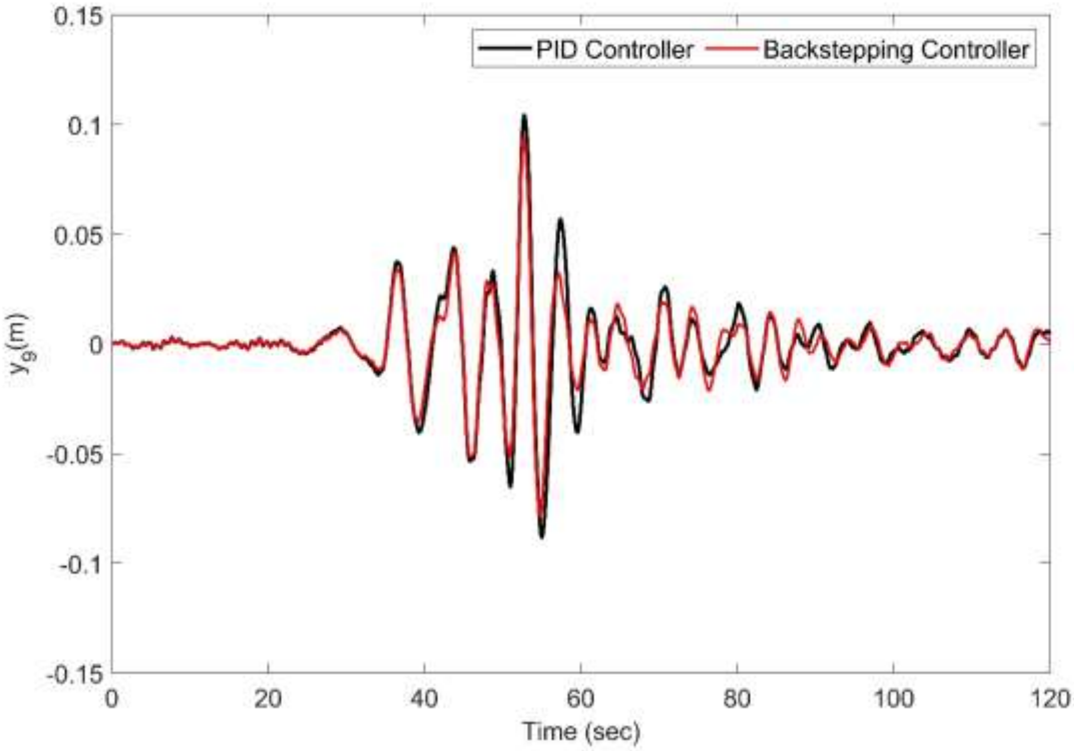

Figure 5. Displacements of the top floor for backstepping controller and PID controller

Figure 5 shows the top floor displacement, which is one of the most important performance outputs when comparing backstepping and PID controllers.

The displacement of the oscillating controller mass due to the force applied by the earthquake and the actuator is given in Figure 6. The control mass moves at a range of 2 meters for both controllers, which are acceptable strokes for such systems. However, the controller mass displacement of the backstepping controller is lower than that of the PID controller.

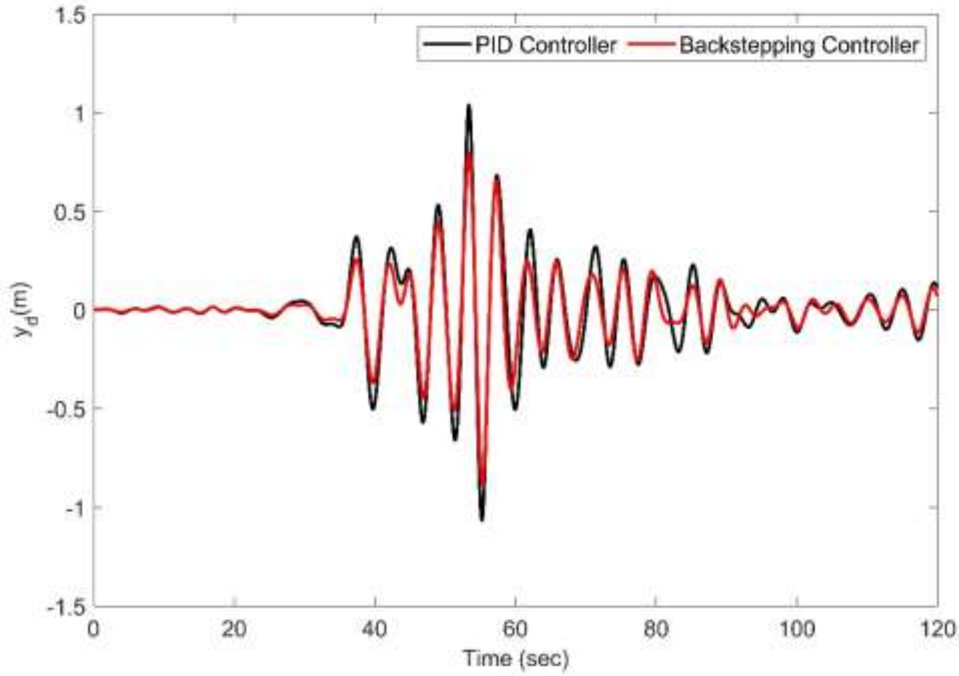

Figure 6. Displacement of controller mass while reaching the control aim for backstepping controller and PID controller

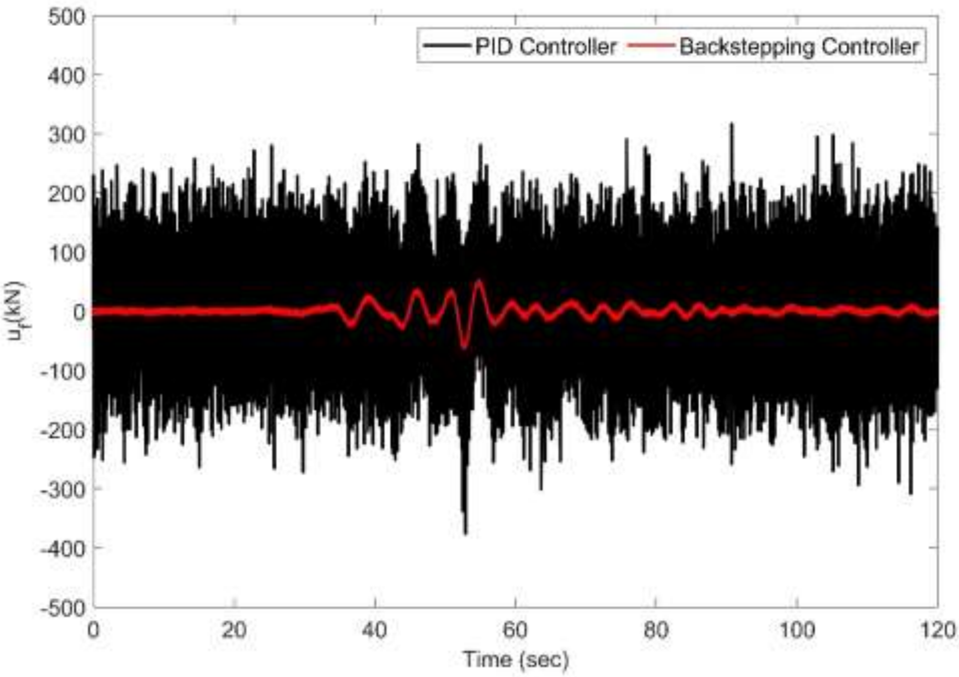

Figure 7. Change of control force needed while reaching control objective for backstepping controller and PID controller

The control force applied to reduce earthquake-induced vibrations in the building is shown in Figure 7. The PID controller required significantly greater control force than the backstepping controller in order to exhibit comparable performance in terms of vibration damping, as seen in Figure 7. This outcome is critical because it plays a big role in actuator choice. It demonstrates that the control goal may be achieved by employing a reduced-capacity actuator in the context of measurement noise and potential sensor accuracy issues.

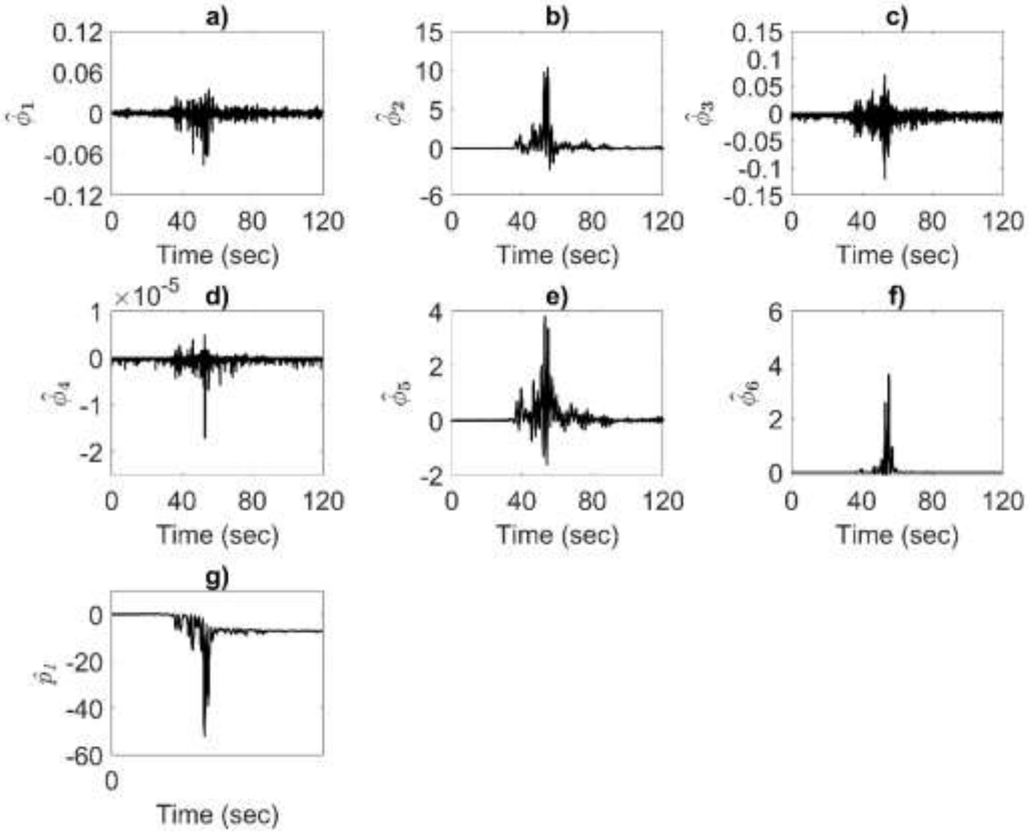

Figure 8. Adaptive compensations of uncertain parameters for Kocaeli Earthquake

Figure 8(a), 8(b), 8(c), 8(d), 8(e), 8(f) and 8(g) show adaptive compensations for uncertain parameters $\hat{\phi}_1, \hat{\phi}_2, \hat{\phi}_3, \hat{\phi}_4, \hat{\phi}_5, \hat{\phi}_6$ and $\hat{p}_1$, respectively. Compensation terms are used to achieve the overall control purpose. The numerical values that these terms have in the process are unimportant, provided they change within a limited range. As shown in Figure 8, while the structural vibrations caused by an earthquake are reduced by using the designed controller in ATMD system, the variation of compensation parameters in a limited range is observed.

The performance results of the adaptive robust backstepping controller compared with the PID controller were tested with performance criteria that have proven itself in the literature to test the performance of the controllers designed for such structures. Twelve performance criteria were defined to evaluate for designed control systems for building structures with ATMD systems by Yang et al., (2001). These evaluation criteria were used in many pioneering studies in the literature to test the performance of ATMD systems (Nagarajaiah & Varadarajan, 2005; Varadarajan & Nagarajaiah, 2004). In this study, these evaluation criteria based on both the peak and root mean square (RMS) responses of the building were adapted for nine-story building. Definitions of these criteria denoted by $J_1 - J_{12}$ are given in Table 2.

Table 2. Evaluation criteria

$J_1 = \frac{\max(\sigma_{\ddot{y}n})}{\sigma_{\ddot{y}9o}}$ *for n=1 to 9*	$J_5 = \frac{\sigma_{yd}}{\sigma_{y9o}}$	$J_9 = \frac{y_{p9}}{y_{p9o}}$
$J_2 = \frac{1}{6}\sum_n(\sigma_{\ddot{y}n}/\sigma_{\ddot{y}no})$ *for n=4,5,6,7,8 and 9*	$J_6 = \left\{\frac{1}{T}\int_0^T [\dot{y}_d(t)u_f(t)]^2 dt\right\}$	$J_{10} = \frac{1}{7}\sum_n(y_{pn}/y_{pno})$ *for n=3,4,5,6,7,8 and 9*
$J_3 = \frac{\sigma_{y9}}{\sigma_{y9o}}$	$J_7 = \frac{\max(\ddot{y}_{pn})}{\ddot{y}_{p9o}}$ *for n=1 to 9*	$J_{11} = \frac{y_{pd}}{y_{p9o}}$
$J_4 = \frac{1}{7}\sum_n(\sigma_{yn}/\sigma_{yno})$ *for n=3,4,5,6,7,8 and 9*	$J_8 = \frac{1}{6}\sum_n(\ddot{y}_{pn}/\ddot{y}_{pno})$ *for n=4,5,6,7,8 and 9*	$J_{12} = \max_t\lvert\dot{y}_d(t)u_f(t)\rvert$

In first criterion J_1, $\sigma_{\ddot{y}n}$ and $\sigma_{\ddot{y}9o}$ represent RMS acceleration of the nth floor and RMS acceleration of the 9th floor for uncontrolled situation, respectively. In J_2, $\sigma_{\ddot{y}no}$denotes RMS acceleration of nth floor for uncontrolled situation. In J_4, σ_{yn} and σ_{yno} represent RMS displacements of nth floor and RMS displacements of nth floor for uncontrolled situation, receptively. In criterion five σ_{yd} specify the RMS displacement of controller mass. In J_6, $\dot{y}_d(t)$ denotes actuator velocity and $u_f(t)$ denotes actuator force. Criteria J_7 to J_{11} are calculated similarly to the first five criteria, but peak values are used instead of RMS values. For each criteria of performance values, less than 1.0 implies an improvement in control response compared with the uncontrolled scenario, except for the J_5, J_6, J_{11}, and J_{12} performance indices (Ümütlü et al., 2022; Varadarajan & Nagarajaiah, 2004).

Table 3 shows the calculated performance criteria of the backstepping controller and the PID controller for the Kocaeli earthquake. Also, RMS and max values of u_f and y_d are given to evaluate the performance of the controllers.

Table 3. Evaluation criteria results of Backstepping and PID controllers for the Kocaeli Earthquake.

	Backstepping Controller	*PID*		*Backstepping Controller*	*PID*
J_1	0.275	0.296	J_7	0.634	0.681
J_2	0.257	0.277	J_8	0.643	0.691
J_3	0.262	0.293	J_9	0.666	0.702
J_4	0.263	0.291	J_{10}	0.659	0.701
J_5	2.551	3.223	J_{11}	5.936	7.183
J_6 $(kN\ m/s)$	6.482	15.961	J_{12} $(kN\ m/s)$	61.619	465.743
$\sigma u_f\ (kN)$	10.420	38.027	$max\|u_f\|\ (kN)$	52.523	316.144
$\sigma_{yd}\ (cm)$	16.549	20.905	$max\|y_d\|\ (cm)$	79.463	103.897

In Table 3, the results of two different controllers tested for the nine-story structure are given for the Kocaeli earthquake. When the results are examined, it is seen that the adaptive backstepping controller gives the better results for the all performance criteria, which are the building acceleration-based (J_1,J_2,J_7, and J_8), displacement based(J_3,J_4,J_5,J_9, J_{10} and J_{11}) and control force based (J_6 and J_{12}) criteria. Especially, as can be seen from the σu_f and $max|u_f|$ results as well as the J_6 and J_{12} parameters that measure the performance in terms of control forces, the backstepping controller has a great advantage.

5. Conclusions

In this study, a controller is designed to mitigate earthquake-induced vibrations of a non-linear multi-story building using ATMD. In addition to structural nonlinearities, band-limited white noise has been applied as a disturbance input on the last floor of the building to represent unknown nonlinear situations such as measurement noise and uncertain dynamics. Adaptive compensation terms are used to design a robust controller independent of structural parameters. Stability of the structure while reaching the control target is guaranteed by a Lyapunov-based stability criterion that handles all nonlinear and unknown situations. With the Lyapunov-based stability analysis described in the paper, it is theoretically guaranteed that the proposed controller will keep the system stable while attaining the main control goal, as long as the constant control gains are chosen as positive numerical values. Owing to the robust structure of the designed controller and the adaptive compensation rules proposed in the study, a general controller structure that can be used in all systems with a similar mathematical model aiming at vibration damping with ATMD systems has been obtained. Simulation experiments in Matlab/Simulink were used to verify the performance of the developed controller. In addition, comparative simulation studies were also carried out. From these results, it is seen that the robust adaptive backstepping controller, which is designed, has achieved its control purpose by requiring much less control effort compared to the widely preferred robust counterpart, PID. The simulation results were evaluated with the evaluation criteria commonly used in the literature. Especially in terms of control force, the designed backstepping controller has a great advantage compared to PID.

References

Adhikari, R., Yamaguchi, H., & Yamazaki, T. (1998). Modal space sliding-mode control of structures. *Earthquake Engineering and Structural Dynamics*, *27*(11), 1303–1314. https://doi.org/10.1002/(SICI)1096-9845(1998110)27:11<1303::AID-EQE785>3.0.CO;2-J

Aghabalaei Baghaei, K., Ghaffarzadeh, H., & Younespour, A. (2019). Orthogonal function-based equivalent linearization for sliding mode control of nonlinear systems. *Structural Control and Health Monitoring*, *26*(8), e2372. https://doi.org/10.1002/stc.2372

Alexander, N. A., & Schilder, F. (2009). Exploring the performance of a nonlinear tuned mass damper. *Journal of Sound and Vibration*, *319*(1–2), 445–462. https://doi.org/10.1016/j.jsv.2008.05.018

Anh, N. D., & Nguyen, N. X. (2012). Extension of equivalent linearization method to design of TMD for linear damped systems. *Structural Control and Health Monitoring*, *19*(6), 565–573.

Chang, C. C., & Poon, C. W. (2010). Nonlinear Identification of Lumped-Mass Buildings Using Empirical Mode Decomposition and Incomplete Measurement. *Journal of Engineering Mechanics*, *136*(3), 273–281. https://doi.org/10.1061/(asce)0733-9399(2010)136:3(273)

Collette, C., & Chesné, S. (2016). Robust hybrid mass damper. *Journal of Sound and Vibration*, *375*, 19–27. https://doi.org/10.1016/j.jsv.2016.04.030

Eason, R. P., Sun, C., Dick, A. J., & Nagarajaiah, S. (2013). Attenuation of a linear oscillator using a nonlinear and a semi-active tuned mass damper in series. *Journal of Sound and Vibration*, *332*(1), 154–166. https://doi.org/10.1016/j.jsv.2012.07.048

Etedali, S., & Tavakoli, S. (2017). PD/PID Controller Design for Seismic Control of High-Rise Buildings Using Multi-Objective Optimization: A Comparative Study with LQR Controller. *Journal of Earthquake and Tsunami*, *11*(3), 1750009. https://doi.org/10.1142/S1793431117500099

Etedali, S., Zamani, A. A., & Tavakoli, S. (2018). A GBMO-based PIλDμ controller for vibration mitigation of seismic-excited structures. *Automation in Construction*, *87*, 1–12. https://doi.org/10.1016/j.autcon.2017.12.005

Fang, J. S., Hai, W. H., & Zhang, X. L. (2001). An analytical study for controlling chaos in Duffing oscillator with weak periodic perturbation. *Chinese Physics Letters*, *18*(3), 334–336. https://doi.org/10.1088/0256-307X/18/3/308

Ghaffarzadeh, H., Younespour, A., & Cheng, S. (2020). Design of a tuned mass damper for damped structures using an orthogonal-function-based equivalent linearization method. *Structures*, *28*, 2605–2616.

Ghandchi-Tehrani, M., Wilmshurst, L. I., & Elliott, S. J. (2015). Bifurcation control of a Duffing oscillator using pole placement. *JVC/Journal of Vibration and Control*, *21*(14), 2838–2851. https://doi.org/10.1177/1077546313517586

Ghandchi Tehrani, M., & Elliott, S. J. (2014). Extending the dynamic range of an energy harvester using nonlinear damping. *Journal of Sound and Vibration*, *333*(3), 623–629. https://doi.org/10.1016/j.jsv.2013.09.035

Guclu, R. (2006). Sliding mode and PID control of a structural system against earthquake. *Mathematical and Computer Modelling*, *44*(1–2), 210–217. https://doi.org/10.1016/j.mcm.2006.01.014

Guclu, R., & Yazici, H. (2008). Vibration control of a structure with ATMD against earthquake using fuzzy logic controllers. *Journal of Sound and Vibration*, *318*(1–2), 36–49. https://doi.org/10.1016/j.jsv.2008.03.058

Gutierrez Soto, M., & Adeli, H. (2013). Tuned Mass Dampers. *Archives of Computational Methods in Engineering*, *20*(4), 419–431. https://doi.org/10.1007/s11831-013-9091-7

Hacioglu, Y., & Yagiz, N. (2012). Adaptive backstepping control with estimation for the vibration isolation of buildings. *JVC/Journal of Vibration and Control*, *18*(13), 1996–2005. https://doi.org/10.1177/1077546311429052

Kayabekir, A. E., Bekdaş, G., Nigdeli, S. M., & Geem, Z. W. (2020). Optimum design of PID controlled active tuned mass damper via modified harmony search. *Applied Sciences*

(Switzerland), 10(8), 2976. https://doi.org/10.3390/APP10082976

Krenk, S. (2005). Frequency analysis of the tuned mass damper. *Journal of Applied Mechanics, Transactions ASME, 72*(6), 936–942. https://doi.org/10.1115/1.2062867

Krstic, M., Kokotovic, P. V, & Kanellakopoulos, I. (1995). *Nonlinear and adaptive control design*. John Wiley & Sons, Inc.

Li, C., & Cao, L. (2019). High performance active tuned mass damper inerter for structures under the ground acceleration. *Earthquake and Structures*, *16*(2), 149–163. https://doi.org/10.12989/eas.2019.16.2.149

Mañosa, V., Ikhouane, F., & Rodellar, J. (2005). Control of uncertain non-linear systems via adaptive backstepping. *Journal of Sound and Vibration*, *280*(3–5), 657–680. https://doi.org/10.1016/j.jsv.2003.12.033

Nagarajaiah, S., & Varadarajan, N. (2005). Short time Fourier transform algorithm for wind response control of buildings with variable stiffness TMD. *Engineering Structures*, *27*(3), 431–441. https://doi.org/10.1016/j.engstruct.2004.10.015

Novak, S., & Frehlich, R. G. (1982). Transition to chaos in the Duffing oscillator. *Physical Review A*, *26*(6), 3660–3663. https://doi.org/10.1103/PhysRevA.26.3660

Preumont, A., Alaluf, D., & Bastaits, R. (2014). Hybrid Mass Damper: A Tutorial Example. *CISM International Centre for Mechanical Sciences, Courses and Lectures*, *558*, 179–211. https://doi.org/10.1007/978-3-7091-1821-4_3

Socha, L., & Blachuta, M. (2000). Application of linearization methods with probability density criteria in control problems. *Proceedings of the 2000 American Control Conference. ACC (IEEE Cat. No. 00CH36334)*, *4*, 2775–2779.

Ümütlü, R. C., Bidikli, B., & Ozturk, H. (2022). A backstepping control design for ATMD systems of building structure against earthquake excitations in the presence of parametric uncertainty. *Structural Control and Health Monitoring*, *29*(3), e2893. https://doi.org/10.1002/stc.2893

Ümütlü, R. C., Ozturk, H., & Bidikli, B. (2021). A robust adaptive control design for active tuned mass damper systems of multistory buildings. *JVC/Journal of Vibration and Control*, *27*(23–24), 2765–2777. https://doi.org/10.1177/1077546320966236

Varadarajan, N., & Nagarajaiah, S. (2004). Wind Response Control of Building with Variable Stiffness Tuned Mass Damper Using Empirical Mode Decomposition/Hilbert Transform. *Journal of Engineering Mechanics*, *130*(4), 451–458. https://doi.org/10.1061/(asce)0733-9399(2004)130:4(451)

Yang, J. N., Agrawal, A. K., Samali, B., & Wu, J. C. (2001). A benchmark problem for response control of wind-excited tall buildings. *Proceedings of the International Modal Analysis Conference - IMAC*, *1*(4), 151–157. https://doi.org/10.1061/(asce)0733-9399(2004)130:4(437)

Yu, W., & Thenozhi, S. (2016). *Active Structural Control with Stable Fuzzy PID Techniques*. Springer. https://doi.org/10.1007/978-3-319-28025-7